



# Multistep synthesis and upconversion luminescence of spherical $\text{Gd}_2\text{O}_3:\text{Er}$ and $\text{Gd}_2\text{O}_3:\text{Er}$ @ silica

Nguyen Thi Quy Hai<sup>1</sup> · Tran Kim Anh<sup>1</sup> · Pham Thi Minh Chau<sup>1</sup> · Vu Thi Thai Ha<sup>2</sup> · Ho Van Tuyen<sup>1</sup> · Tran Thu Huong<sup>2,4</sup> · Ha Thi Phuong<sup>3</sup> · Quoc Le Minh<sup>1</sup>

Received: 17 June 2019 / Accepted: 6 January 2020 / Published online: 17 January 2020  
© Springer Science+Business Media, LLC, part of Springer Nature 2020

## Abstract

Spherical  $\text{Gd}_2\text{O}_3:\text{Er}^{3+}$  and  $\text{Gd}_2\text{O}_3:\text{Er}^{3+}$  @ silica nanoparticles have been successfully synthesized by a multistep procedure including precipitation and sol–gel processes from rare-earth nitrates, TEOS and urea as starting precursors. The structure, morphology and chemical composition of the products were characterized by X-ray diffraction, field emission scanning electron microscopy, and fourier transform infrared spectroscopy. The results indicated that the obtained phosphors consist of separated, non-agglomerated spheres in nanoscale with an uniform, ideal spherical shape. The suitable amount of TEOS was addressed to obtain the spherical  $\text{Gd}_2\text{O}_3:\text{Er}^{3+}$  @ silica nanocomposites with the luminescence intensity almost unchanged with respect to the uncoated  $\text{Gd}_2\text{O}_3:\text{Er}^{3+}$  sample. Besides, the upconversion emission spectra showed intense green and red emission bands under 980-nm laser diode excitation with remarkable increase in the red emissions. The upconversion luminescence followed the two-photon mechanism for green and red emissions. With obtained results, the prepared nanospheres are expected to be a potential material to create functional groups for subsequent bio-conjugation with various biomolecules in medical diagnostics.

## 1 Introduction

Rare-earth ion (RE)-doped inorganic luminescent nanomaterials are important and interesting subjects for fundamental research and applications in many fields of technology. Among these materials,  $\text{Gd}_2\text{O}_3:\text{Er}^{3+}$  is widely known as a high-efficient oxide phosphor and attracted much attention of researchers worldwide.  $\text{Gd}_2\text{O}_3$  is usually used as a host matrix for doping with various rare-earth ions [1].  $\text{Er}^{3+}$  ion is an attractive activator for achieving intense emission in

green and red spectral regions [2], especially for preparation of converting luminescence materials [3, 4]. Owing to these advantages,  $\text{Gd}_2\text{O}_3:\text{Er}^{3+}$  nanoparticles have been intensively investigated and found a wide range of applications. Several methods have been applied for synthesis of the  $\text{Gd}_2\text{O}_3$  nanoparticles (NPs), undoped or doped with RE ions. Many interesting systems of nanomaterials have also been investigated for different application purposes [5–7]. Besides that, the energy levels of  $\text{Er}^{3+}$  ion in  $\text{Gd}_2\text{O}_3$  matrix, the energy transfers in  $\text{Er}^{3+}$ -doped  $\text{Gd}_2\text{O}_3$  NPs, as well as the luminescence conversion effect, color tunability of  $\text{Gd}_2\text{O}_3$ ,  $\text{Gd}_2\text{O}_3:\text{Er}^{3+}$  and  $\text{Gd}_2\text{O}_3:\text{Er}^{3+}/\text{Yb}^{3+}$  were the subjects of many investigations [8–10].

Recently, much effort has been made in term of the usage of the  $\text{Ln}^{3+}$ -doped fluorescent compounds in biomedicine based on their excellent optical properties, such as sharp emission lines, long lifetimes and photo-stability [11, 12]. For this purpose, a perfect spherical shape, narrow size distribution, and non-agglomeration of material are required. Under these conditions, the phosphor shows high brightness, high-resolution, and low-light scattering [13]. So far, many synthetic routes focused on controlling the spherical shape, size and distribution of phosphor particles, such as hydrothermal synthesis of  $\text{Y}_2\text{O}_3:\text{Yb}^{3+}/\text{Er}^{3+}$  nanospheres

✉ Nguyen Thi Quy Hai  
nguyenquyhaivie@yahoo.com

- <sup>1</sup> Institute of Theoretical and Applied Research, Duy Tan University, T2-CT1, Trang An Complex, Phung Chi Kien, Hanoi 100000, Vietnam
- <sup>2</sup> Institute of Materials Science, Vietnam Academy of Science and Technology, 18 Hoang Quoc Viet, Cau Giay, Hanoi 100000, Vietnam
- <sup>3</sup> Department of Chemistry, Hanoi Medical University, 1 Ton That Tung, Hanoi 100000, Vietnam
- <sup>4</sup> Graduate University of Science and Technology, Vietnam Academy of Science and Technology, 18 Hoang Quoc Viet, Cau Giay, Hanoi 100000, Vietnam

with upconversion luminescence [13], aging at elevated temperature for preparation of monodispersed colloidal particles of lanthanide compounds [14], chemical precipitation for preparation of core-shell  $\text{Gd}_2\text{O}_3:\text{Eu}$  @  $\text{mSiO}_2$  hollow nanospheres for drug release [15, 16], sol-gel process for creating  $\text{SiO}_2$  layer onto the surface of nanophosphor [17, 18], etc. Although many efforts have been made, to our knowledge, the synthesis of nanospheres with controllable shape and size and their properties has been relatively less studied in comparison with the nanopowder materials fabricated by solid-state reaction or combustion methods. In addition, the surface modification and functionalization are always needed to make the phosphor useful for further application. Silica [ $\text{SiO}_{2-x}(\text{OH})_x$ ] is an excellent candidate for modifying the surface of phosphors because of its high dispersion. The OH groups on silica matrix give the surface hydrophilic properties, make it better dispersed in different solvents. Then, the structure can be easily functionalized to develop high-resolution optical imaging in biomedical diagnose. In our previous publication [19], we have reported the optical properties of  $\text{Gd}_2\text{O}_3:\text{Er}^{3+}$  nanopowders fabricated by EDTA-assisted combustion method and their composite structures formed by coating the NPs with silica.

To continue this research, we focused on  $\text{Gd}_2\text{O}_3:\text{Er}$  nanosphere in this work. We applied with great modify the chemical precipitation method for synthesis of uniform  $\text{Gd}_2\text{O}_3:\text{Er}^{3+}$  NSPs followed by the coating  $\text{Gd}_2\text{O}_3:\text{Er}^{3+}$  with silica using the sol-gel method to obtain  $\text{Gd}_2\text{O}_3:\text{Er}^{3+}$  @  $\text{SiO}_2$  nanospheres. This method is simple, low cost, high efficiency and environmental friendly. Using an appropriate synthesis procedure following a careful stepwise heat-treating regime we intend to obtain  $\text{Gd}_2\text{O}_3:\text{Er}^{3+}$  and  $\text{Gd}_2\text{O}_3:\text{Er}^{3+}$  @ silica nanospheres with sufficient luminescent and structural properties, so that can be useful for application in medical field. The crystalline phase identification, morphology, chemical composition and luminescence properties of the products have been investigated and discussed.

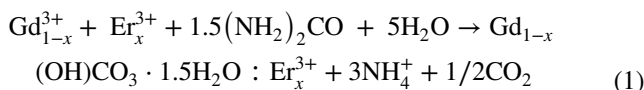
## 2 Experimental details

### 2.1 Materials

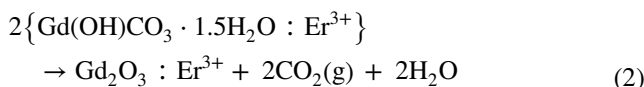
The initial chemicals including  $\text{Gd}(\text{NO}_3)_3 \cdot 6\text{H}_2\text{O}$  99.9% (Sigma-Aldrich),  $\text{Er}(\text{NO}_3)_3 \cdot 5\text{H}_2\text{O}$  99.9% (Sigma-Aldrich), TEOS [ $(\text{C}_2\text{H}_5\text{O})_4\text{Si}$ ] 99.9% (Sigma-Aldrich), urea [ $\text{CO}(\text{NH}_2)_2$ ] 99.8% (Prolabo), and  $\text{HNO}_3$  65 wt%,  $\text{NH}_4\text{OH}$  28 wt%, absolute  $\text{C}_2\text{H}_5\text{OH}$  (all with purity of A.R) were used without further purification.

### 2.2 Synthesis of $\text{Gd}(\text{OH})\text{CO}_3 \cdot \text{H}_2\text{O}:\text{Er}^{3+}$ and $\text{Gd}_2\text{O}_3:\text{Er}^{3+}$ nanospheres

To synthesize the  $\text{Gd}_2\text{O}_3:\text{Er}^{3+}$  nanospheres, the  $\text{Gd}(\text{OH})\text{CO}_3 \cdot \text{H}_2\text{O}:\text{Er}^{3+}$  NSPs were first prepared via homogeneous precipitation. Urea served as a precipitation agent because it can self-decomposes into the  $\text{OH}^-$  and  $\text{CO}_3^{2-}$  at temperature of about 83 °C [16, 20]. It is a simple and often been used method for preparation of lanthanide oxide phosphors. In a typical synthesis, the stoichiometric volume of 0.4 M  $\text{Gd}(\text{NO}_3)_3 \cdot 6\text{H}_2\text{O}$  and 0.1 M  $\text{Er}(\text{NO}_3)_3 \cdot 5\text{H}_2\text{O}$  solutions in DI water were mixed in a 150 ml glass bottle and stirred during 15 min to form homogeneous and clear solution. A necessary amount of urea, calculated from the selected molar ratio of the amount of urea and total amount of rare-earth ions, denoting as urea/ $[\text{Gd}^{3+} + \text{Er}^{3+}]$  molar ratio, was dissolved in 100 ml DI water, then the mixed RE solution was added dropwise to the urea solution by continuous stirring in 2 h at room temperature. The pH of the reaction solution was adjusted and kept at 6.5 using  $\text{NH}_4\text{OH}$  solution during the reaction time. The temperature of the reaction solution was then slowly raised up to 85 °C and kept constant for 2.5 h in an oil bath. The formation of  $\text{Gd}(\text{OH})\text{CO}_3 \cdot \text{H}_2\text{O}:\text{Er}^{3+}$  occurred according to the following reaction:



After the precipitation was completed, the reaction solution was quickly cooled down to room temperature and then has been centrifuged to separate the precipitate. The precipitate was washed with ethanol and DI water, dried in air at 70 °C for 24 h, at 105 °C for 2 h and at 150 °C for 2 h. In these synthetic experiments, the concentration of  $\text{Er}^{3+}$  ion was 1.5, 1.8 and 2.0 mol%. The optimized urea/ $[\text{Gd}^{3+} + \text{Er}^{3+}]$  molar ratio of 25/1 was selected according to previous experience [21]. The reaction products were dry white spherical  $\text{Gd}(\text{OH})\text{CO}_3 \cdot \text{H}_2\text{O}:\text{Er}^{3+}$  particles. One part of the product had undergone a stepwise sintering process at 200 °C for 2 h, at 400 °C for 2 h, at 600 °C for 2 h and at 650 °C for 3 h resulting in the formation of  $\text{Gd}_2\text{O}_3:\text{Er}^{3+}$  oxide spheres [16, 20, 21].



The other part served as starting material for coating with silica shell.

### 2.3 Synthesis of $\text{Gd}(\text{OH})\text{CO}_3 \cdot \text{H}_2\text{O}:\text{Er}^{3+}$ @ silica and $\text{Gd}_2\text{O}_3:\text{Er}^{3+}$ @ silica nanospheres

Similar to the synthesis of  $\text{Gd}_2\text{O}_3:\text{Er}^{3+}$  NSPs, the synthesis of  $\text{Gd}_2\text{O}_3:\text{Er}^{3+}$  @ silica NSPs consists two steps: The first

step is preparation of  $\text{Gd}(\text{OH})\text{CO}_3 \cdot \text{H}_2\text{O} \cdot \text{Er}^{3+}$  @ silica particles by sol–gel method and the next step is the calcination process to convert  $\text{Gd}(\text{OH})\text{CO}_3 \cdot \text{H}_2\text{O} \cdot \text{Er}^{3+}$  @ silica into  $\text{Gd}_2\text{O}_3 \cdot \text{Er}^{3+}$  @ silica nanospheres. In the first step, 150 mg of  $\text{Gd}(\text{OH})\text{CO}_3 \cdot \text{H}_2\text{O} \cdot \text{Er}^{3+}$  were well dispersed in a mixed solution of 150 ml of absolute  $\text{C}_2\text{H}_5\text{OH}$  and 60 ml of DI water by ultra-sonication for 60 min. 150  $\mu\text{l}$  of tetraethoxysilane (TEOS) dispersed in 10-ml ethanol was added dropwise, followed by adding 1.0 ml of  $\text{NH}_4\text{OH}$  (28 wt%). The solution was then continuously stirred for 24 h at room temperature. After that, the solution was heated to 60 °C and kept for 60 min. Then, it was cooled down to room temperature and the formed particles were separated, washed until pH 7 and dried subsequently at 70 °C for 24 h, at 105 °C for 2 h and at 150 °C for 2 h. The further heat-treating regime included heating at 200 °C for 2 h, at 400 °C for 2 h, at 600 °C for 2 h, and at 650 °C for 3 h, subsequently. The final product was  $\text{Gd}_2\text{O}_3 \cdot \text{Er}^{3+}$  @ silica nanospheres. The same procedure has been applied for the synthesis of the sample with 200- $\mu\text{l}$  TEOS.

## 2.4 Characterization

The structure and morphology of all samples were investigated using a Bruker D8-Advance diffractometer, and field emission scanning electron microscopy (FESEM, model: Hitachi S-4800). Functional groups were measured with the aid of a fourier transform infrared spectrometer (FTIR, Model Fourier NEXUS 670). The PL spectra and the PL excitation (PLE) spectra of all samples were recorded using a FL 3–22 HORIBA spectrometer with double monochromators. Upconversion luminescent spectra were measured on an iHR 550 (Jobin-Yvon) equipment using 980-nm laser diode (LD) excitation.

## 3 Results and discussions

### 3.1 Structure and morphology

The XRD analysis reveals that the as-prepared  $\text{Gd}(\text{OH})\text{CO}_3 \cdot \text{H}_2\text{O} \cdot \text{Er}^{3+}$  nanospheres after drying at 200 °C is amorphous (figure not shown). This result is coincident with the previous reports [16, 20]. Thermal decomposition via calcinations at 650 °C for 3 h results in the conversion of amorphous  $\text{Gd}(\text{OH})\text{CO}_3 \cdot \text{H}_2\text{O} \cdot \text{Er}^{3+}$  to  $\text{Gd}_2\text{O}_3 \cdot \text{Er}^{3+}$  crystalline material. The XRD pattern pointed out the pure cubic phase of gadolinium oxide (JCPDS Card No. 43-1014), as shown in Fig. 1a. Besides that, the broadening of XRD peaks was observed suggesting the formation of nano-sized crystallites. Using Scherrer formula, the crystallite size of these nanocrystals was calculated to be 40 nm in average. Moreover, FESEM image of  $\text{Gd}(\text{OH})\text{CO}_3 \cdot \text{H}_2\text{O} \cdot \text{Er}^{3+}$  nanospheres is shown in Fig. 1b. It indicated that the as-prepared  $\text{Gd}(\text{OH})\text{CO}_3 \cdot \text{H}_2\text{O} \cdot \text{Er}^{3+}$  nanospheres have spherical shape with smooth surface and homogeneously monodispersed. The grain size estimated from FESEM image ranges from 200 to 250 nm. After calcinations at high temperature (650 °C for 3 h), amorphous  $\text{Gd}(\text{OH})\text{CO}_3 \cdot \text{H}_2\text{O} \cdot \text{Er}^{3+}$  nanospheres were thermal decomposed and  $\text{Gd}_2\text{O}_3 \cdot \text{Er}^{3+}$  crystalline phase was formed instead [13]. The spherical shape was remained, as shown in Fig. 2a. It was the result of our careful stepwise heat treatment regime. After being annealed at 650 °C for 3 h, the average spheres size reduced remarkably to 80 nm of uncoated  $\text{Gd}_2\text{O}_3 \cdot \text{Er}^{3+}$  sphere, estimated from FESEM image (Fig. 2a), and is almost twice the crystallite size determined from XRD data. This discrepancy can be explained by the fact that

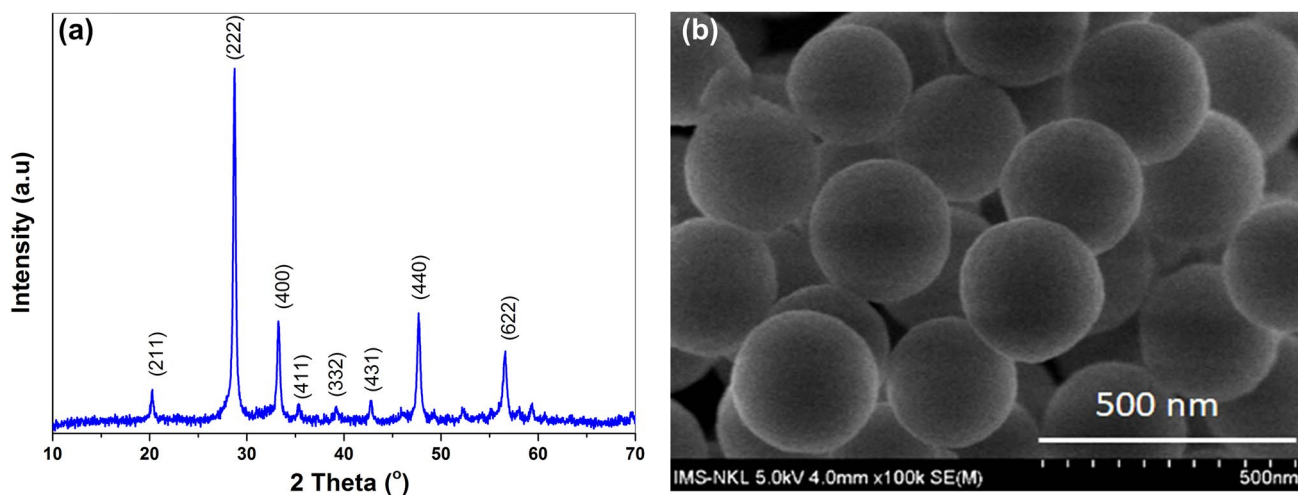


**Fig. 1** XRD patterns of  $\text{Gd}_2\text{O}_3 \cdot \text{Er}^{3+}$  1.8 mol% nanosphere material annealed at 650 °C for 3 h (a); FESEM image of  $\text{Gd}(\text{OH})\text{CO}_3 \cdot \text{H}_2\text{O} \cdot \text{Er}^{3+}$  2 mol%, dried at 150 °C 2 h (b)

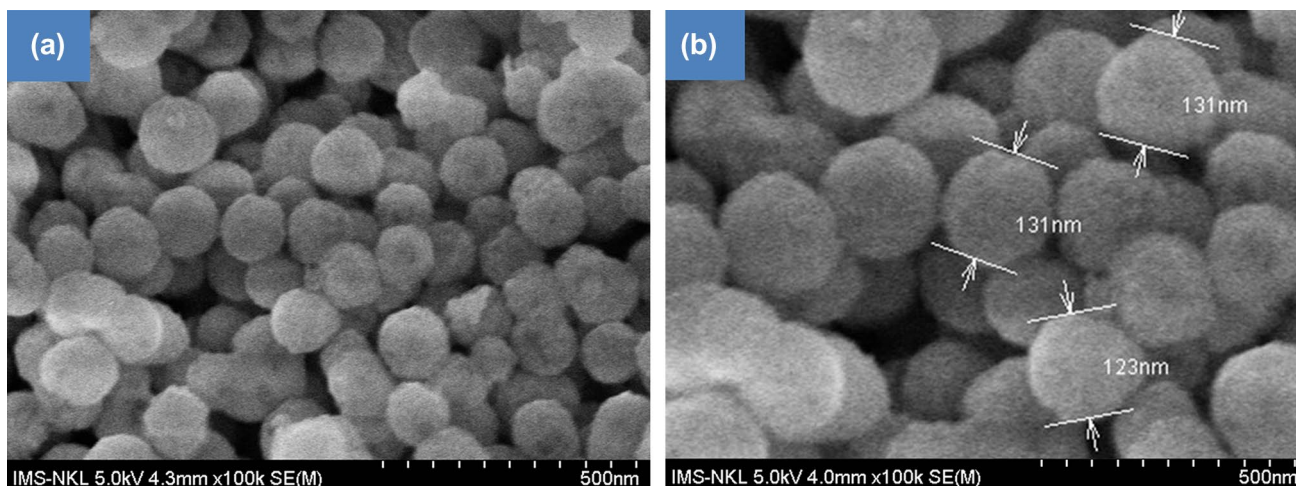


**Fig. 2** FESEM image of  $\text{Gd}_2\text{O}_3:\text{Er}^{3+}$  2 mol % uncoated at  $650^\circ\text{C}$ , 3 h (a);  $\text{Gd}_2\text{O}_3:\text{Er}^{3+}$  2 mol% @ silica (200  $\mu\text{l}$  TEOS), at  $650^\circ\text{C}$ , 3 h (b)

the spherical grains observed in FESEM image might comprised of smaller crystallites, similar to the case reported in Ref. [1]. Figure 2b gives the FESEM image of  $\text{Gd}_2\text{O}_3:\text{Er}^{3+}$  2 mol% @ silica (200  $\mu\text{l}$  TEOS) obtained after calcining the  $\text{Gd}(\text{OH})\text{CO}_3\cdot\text{H}_2\text{O}:\text{Er}^{3+}$  2 mol% @ silica (200  $\mu\text{l}$  TEOS) NSPs at  $650^\circ\text{C}$  for 3 h. One can see that the spherical core  $\text{Gd}_2\text{O}_3:\text{Er}^{3+}$  has been homogeneously coated with a silica layer. The reason for the easy reaction of TEOS with the core surface to form homogeneous silica layer is the hydrated phase and the presence of  $\text{OH}^-$  groups in sol–gel process [20]. The average size of  $\text{Gd}_2\text{O}_3:\text{Er}^{3+}$  2 mol% @ silica spheres estimated from FESEM image was about 130 nm.

### 3.2 Chemical composition

FTIR spectroscopy was performed to qualitatively investigate the chemical composition and chemical bonding of the products. The FTIR spectra of the uncoated and silica-coated  $\text{Gd}_2\text{O}_3:\text{Er}^{3+}$  2 mol% samples are shown in Fig. 3. In the case of uncoated  $\text{Gd}_2\text{O}_3:\text{Er}^{3+}$  NSPs the bands at around 545, 688 and  $757\text{ cm}^{-1}$  can be assigned to the Gd–O vibration of gadolinium oxide and the peak at  $1633\text{ cm}^{-1}$  probably corresponds to the Er–O vibration [2, 19, 22]. This confirmed the formation of the  $\text{Er}^{3+}$ -doped  $\text{Gd}_2\text{O}_3$  nanocrystals. In the FTIR spectra of silica-coated  $\text{Gd}_2\text{O}_3:\text{Er}^{3+}$  2 mol% NSPs an additional characteristic absorption band of Si–O–Si group was clearly seen around  $1082\text{ cm}^{-1}$  [23], which confirmed the formation of  $\text{Gd}_2\text{O}_3:\text{Er}^{3+}$  @ silica structure. The band at approximately  $3400\text{ cm}^{-1}$  revealed the presence of  $\text{OH}^-$  groups from surface absorbed  $\text{H}_2\text{O}$  and hydroxide molecules.

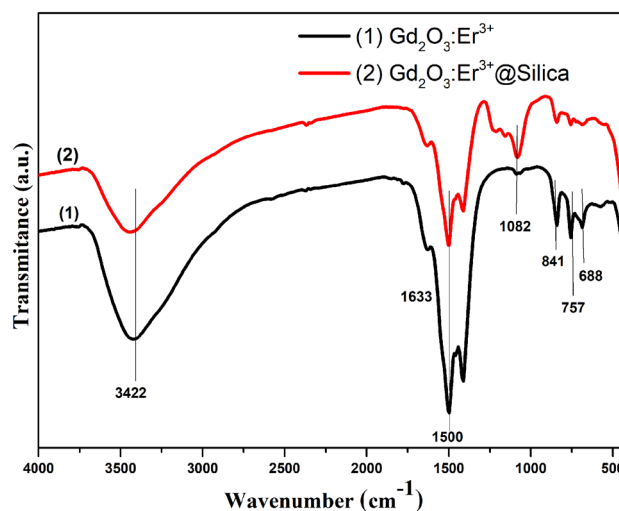


**Fig. 3** FTIR spectra of uncoated  $\text{Gd}_2\text{O}_3:\text{Er}^{3+}$  2 mol% and silica-coated  $\text{Gd}_2\text{O}_3:\text{Er}^{3+}$  2 mol% samples

### 3.3 Optical properties

Photoluminescence behavior of the samples have been investigated to elucidate the energy levels and transitions of  $\text{Er}^{3+}$  ions in  $\text{Gd}_2\text{O}_3$  matrix. The photoluminescence excitation spectrum (PLE) of prepared  $\text{Gd}_2\text{O}_3:\text{Er}^{3+}$  2 mol% NSPs annealed at  $650^\circ\text{C}$  for 3 h, monitoring at  $\lambda_{\text{em}} = 562\text{ nm}$  (shown in Fig. 4a) indicates that one can use the wavelengths of 275 or 379 nm for excitation of the  $\text{Gd}_2\text{O}_3:\text{Er}^{3+}$  nanophosphors. The strongest peak was at 379 nm. Figure 4b.1 presents the photoluminescence emission spectrum (PL) of the same sample under 275-nm excitation. This excitation activated the  $^8\text{S}_{7/2}$  to  $^6\text{I}_{7/2}$  state of  $\text{Gd}^{3+}$  ion. The spectrum consists characteristic emission bands of  $\text{Er}^{3+}$  ion in the blue-green, green and red spectral regions, corresponding

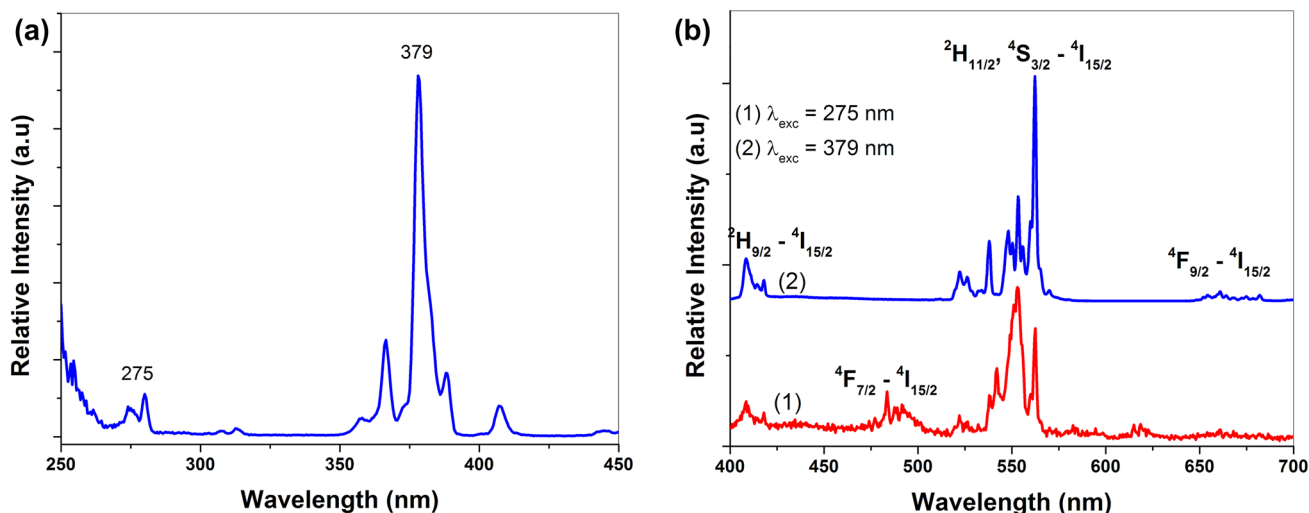


**Fig. 4** PLE spectrum of  $\text{Gd}_2\text{O}_3:\text{Er}^{3+}$  2 mol% NSPs, annealed at  $650^\circ\text{C}$  for 3 h, with monitoring at 562 nm (a); The PL spectra of  $\text{Gd}_2\text{O}_3:\text{Er}^{3+}$  2 mol%, with different wavelength excitations (275 and 379 nm) (b)

to the transitions from  $\text{Er}^{3+}{}^2\text{H}_{9/2} \rightarrow {}^4\text{I}_{15/2}$  (409 nm),  ${}^4\text{F}_{7/2} \rightarrow {}^4\text{I}_{15/2}$  (483 nm),  ${}^2\text{H}_{11/2} \rightarrow {}^4\text{I}_{15/2}$  (542 nm),  ${}^4\text{S}_{3/2} \rightarrow {}^4\text{I}_{15/2}$  (553 and 562 nm) and  ${}^4\text{F}_{9/2} \rightarrow {}^4\text{I}_{15/2}$  (around 661 nm), respectively. The strongest peak positioned at 553 nm. According to the energy level diagram of  $\text{Er}^{3+}$  ions in  $\text{Gd}_2\text{O}_3:\text{Er}^{3+}$  NPs (Fig. 7a), by absorption of the UV light of 275 nm the ground state of  $\text{Gd}^{3+}$  ion  ${}^8\text{S}_{7/2}$  excites to  ${}^6\text{I}_{7/2}$  energy state. The  ${}^6\text{I}_{7/2}$  state converted  ${}^6\text{P}_{7/2}$  by non-radiative decay. Then, the energy from  ${}^6\text{P}_{7/2}$  level of the  $\text{Gd}^{3+}$  ion transferred to the  ${}^2\text{P}_{3/2}$  level of the nearby  $\text{Er}^{3+}$  ion and non-radiatively transferred to the lower levels of the  $\text{Er}^{3+}$  ion, giving the visible emissions of the phosphor [24]. The emission spectrum of  $\text{Gd}_2\text{O}_3:\text{Er}^{3+}$  2 mol% NSPs under 379-nm excitation was shown in Fig. 4b.2. The emissions correspond to the transitions of  $\text{Er}^{3+}$  energy levels, namely,  ${}^2\text{H}_{9/2} \rightarrow {}^4\text{I}_{15/2}$  (409 nm),  ${}^2\text{H}_{11/2}$  (522, 538 nm),  ${}^4\text{S}_{3/2}$  (548, 553, 562 nm) and  ${}^4\text{F}_{9/2}$  (around 661 nm) to the ground energy state  ${}^4\text{I}_{15/2}$  were observed. The results of PL analysis show that the prepared samples exhibit high-luminescence efficiency. We also noted that the  $\text{Gd}_2\text{O}_3:\text{Er}^{3+}$  1.8 mol% sample exhibits the higher value of luminescent intensity than those of the others and will be used for further investigations.

As mentioned above, the spherical  $\text{Gd}_2\text{O}_3:\text{Er}^{3+}$  @ silica composite structure has been achieved by means of homogeneous precipitation combined with sol–gel method using TEOS as silica source. The sol–gel method is well known as a main synthesis technique for creating a silica layer deposited on the surface of nanomaterials to modify, protect their surface and enhance the quality of nanophosphors. The TEOS concentrations of 150  $\mu\text{l}$  and 200  $\mu\text{l}$  were used based on previous experience [21]. Figure 5 presents the PL spectra of uncoated  $\text{Gd}_2\text{O}_3:\text{Er}^{3+}$  1.8 mol% after 3 h of heating at  $650^\circ\text{C}$  and of  $\text{Gd}_2\text{O}_3:\text{Er}^{3+}$  1.8 mol% coated by 150  $\mu\text{l}$

and 200  $\mu\text{l}$  TEOS, heated for 3 h at  $650^\circ\text{C}$ , recorded at room temperature, excited by 379-nm wavelength. We can see that the spectra of  $\text{Gd}_2\text{O}_3:\text{Er}^{3+}$  1.8 mol% @ silica display similar emission bands to uncoated  $\text{Gd}_2\text{O}_3:\text{Er}^{3+}$ , which indicated the similar transitions process of  $\text{Er}^{3+}$  ion in  $\text{Gd}_2\text{O}_3$  host matrix. The emission intensities of coated samples slightly decreased. That can be explained by comparing the above-mentioned XRD patterns of  $\text{Gd}_2\text{O}_3:\text{Er}^{3+}$  and  $\text{Gd}_2\text{O}_3:\text{Er}^{3+}$  @ silica samples. Accordingly, the XRD patterns show that both samples after heating at  $650^\circ\text{C}$  for 3 h remained the cubic crystal structure, so this reduction should be due to the effect of the silica layer deposited onto the surface of NSPs

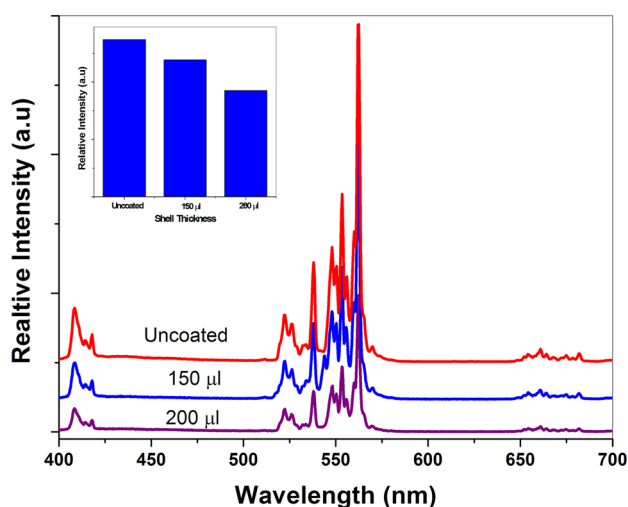


**Fig. 5** PL spectra of  $\text{Gd}_2\text{O}_3:\text{Er}^{3+}$  uncoated, coated with 150- $\mu\text{l}$  TEOS and coated with 200- $\mu\text{l}$  TEOS. The inset shows the PL intensity as a function of the thickness of the TEOS

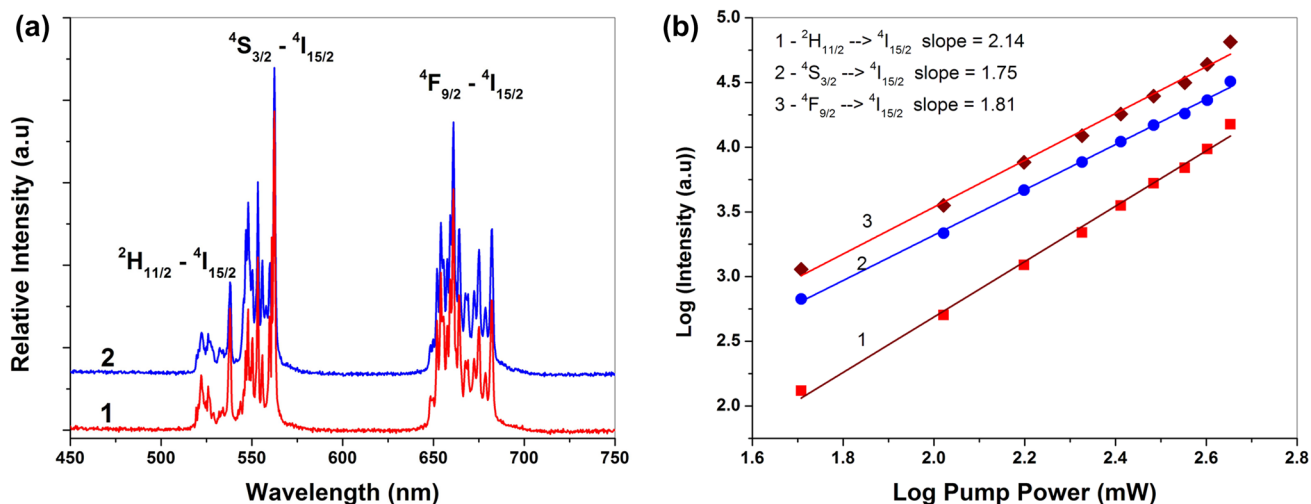
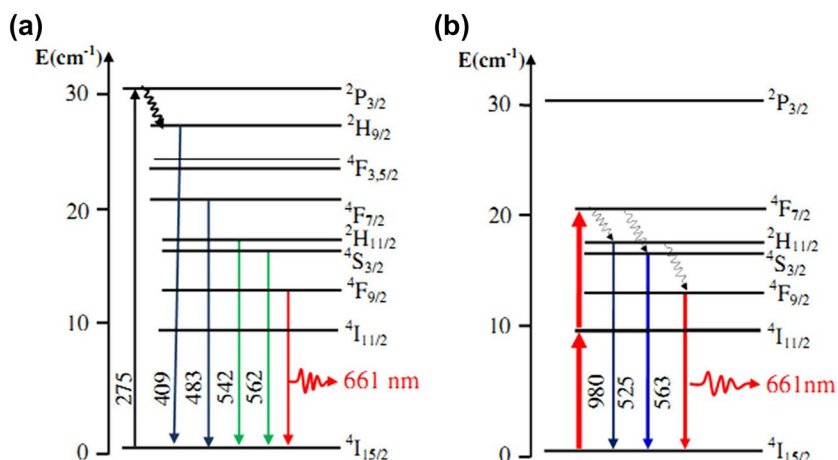


**Fig. 6** UCL spectra of  $\text{Gd}_2\text{O}_3:\text{Er}^{3+}$  1.8 mol% uncoated (red curve) and coated with 150  $\mu\text{l}$  TEOS (blue curve) with  $\lambda_{\text{exc}} = 980$  nm (a);  $I_{\text{pl}}$  versus pump power of  $\text{Gd}_2\text{O}_3:\text{Er}^{3+}$  1.8 mol% (b) (Color figure online)

**Fig. 7** Energy diagram of  $\text{Er}^{3+}$  in  $\text{Gd}_2\text{O}_3$  for PL emissions,  $\lambda_{\text{exc}}$  275 nm (a) and for upconversion emissions  $\lambda_{\text{exc}}$  980 nm (b)



and probably related to the presence of more OH group in coated samples [25]. It may have raised defects on the surface of  $\text{Gd}_2\text{O}_3:\text{Er}^{3+}$  nanoparticles. Our results are in good agreement with observations previously reported [15, 17]. It is worthy to point out from Fig. 5 that the sample coated with 150- $\mu\text{l}$  TEOS gives a luminescence intensity nearly that of the uncoated sample. It means that we selected a suitable  $\text{SiO}_2$  thickness to hinder the decrease of PL intensity of sample. Although the silica coating of the surface of materials may cause a slight decrease in their luminescence intensity, however, luminescent nanomaterials with perfect spherical shape, coated by silica with an appropriate thickness are always preferred for many applications, especially in biomedicine as a targeting drug-delivery structures, etc.

**Upconversion luminescence:** Fig. 6a presents the emission spectra of the  $\text{Gd}_2\text{O}_3:\text{Er}^{3+}$  1.8 mol% (red curve) and

$\text{Gd}_2\text{O}_3:\text{Er}^{3+}$  1.8 mol% @ silica (150  $\mu\text{l}$  TEOS) (blue curve), annealed stepwise up to 650  $^\circ\text{C}$  for 3 h recorded in the range of 450–750 nm, under 980-nm LD excitation. The spectrum show a strong red light, including many bright red emissions of  $\text{Er}^{3+}$  near 661 nm, corresponding to  $\text{Er}^{3+}$   $^4\text{F}_{9/2} \rightarrow ^4\text{I}_{15/2}$  transition together with strong green emission bands centered at 525, 558 and 563 nm assigned to  $\text{Er}^{3+}$   $^2\text{H}_{11/2} \rightarrow ^4\text{I}_{15/2}$ ,  $^4\text{S}_{3/2} \rightarrow ^4\text{I}_{15/2}$  transitions, respectively. The UCL spectra of silica-coated  $\text{Gd}_2\text{O}_3:\text{Er}^{3+}$  1.8 mol% sample is almost the same as that of  $\text{Gd}_2\text{O}_3:\text{Er}^{3+}$  1.8 mol% uncoated sample, except a little lower intensity, which should be ascribed to silica coating. It is worth to note the remarkable enhancement of the red emissions in both  $\text{Gd}_2\text{O}_3:\text{Er}^{3+}$  @ silica or uncoated samples obtained by the procedure described above. They are stronger in comparison with the red emissions of  $\text{Gd}_2\text{O}_3:\text{Er}^{3+}$  nanopowder obtained

by the combustion method [19]. This phenomenon may relate to the location of  $\text{Er}^{3+}$  and the population of the  $^4\text{F}_{9/2}$  red-emitting levels [13]. The strong red emission materials provide various application possibilities in biomedicine and biosensors. The dependence of the emission intensities on the laser diode pump power for the red and green emissions under 980-nm excitation in  $\text{Gd}_2\text{O}_3:\text{Er}^{3+}$  1.8 mol% nanospheres is shown in Fig. 6b. The intensity of the emission bands linearly related to the pump power. The calculated values of slope 'n' indicated that the upconversion process of the samples was two photons transitions for green and red emissions. More clearly, Fig. 7 presents the observed energy levels, excitation and emission transitions of all investigated samples. All the emission bands are assigned to the transition between the energy levels of the  $\text{Er}^{3+}$  ion. Any pair of energy levels in Fig. 7 with closely matching energies bears a potential for energy transfer.

## 4 Conclusions

Using a multistep synthesis procedure, the monodispersed spherical  $\text{Gd}_2\text{O}_3:\text{Er}^{3+}$  and  $\text{Gd}_2\text{O}_3:\text{Er}^{3+}$  @ silica nanoparticles (NSPs) were obtained. The employing of a careful stepwise heating procedure ensures to obtain the products with perfect spherical shape. Both uncoated and silica-coated  $\text{Gd}_2\text{O}_3:\text{Er}^{3+}$  nanospheres exhibited not only downconversion but also upconversion luminescence properties. Especially, with the tetraethoxysilane amount of 150  $\mu\text{l}$ , the luminescence intensity of the spherical  $\text{Gd}_2\text{O}_3:\text{Er}^{3+}$  @ silica nanocomposites is comparable to that of the uncoated  $\text{Gd}_2\text{O}_3:\text{Er}^{3+}$  sample. Possessing ideal spherical shape, strong luminescence emissions, especially high red upconversion emission, the synthesized  $\text{Gd}_2\text{O}_3:\text{Er}^{3+}$ -based luminescent nanoparticles can be subjected to further studies in many fields, especially in sensing and biomedicine.

## References

1. I. Kaminska, D. Elbaum, B. Sikora, P. Kowalik, J. Mikulski, Z. Felcyn, P. Samol, T. Wojciechowski, R. Minikayev, W. Paszkowicz, W. Zaleszczyk, M. Szweczyk, A. Konopka, G. Gruzeł, M.

- Pawlyta, M. Donten, K. Ciszak, K. Zajdel, M. Frontczak-Baniewicz, P. Stępień, M. Łapiński, G. Wilczyński, K. Fronc, *Nanotechnology* **29**, 025702 (2018)
2. Y.A. Kuznetsova, A.F. Zatsepin, V.A. Mashkovtsev, V.N. Rychkov, *IOP Conf. Ser. J. Phys. Conf. Ser.* **917**, 052015 (2017)
3. K. Zheng, Z. Liu, Y. Liu, W. Song, W. Qin, *J. Appl. Phys.* **114**, 183109 (2013)
4. X. Chen, E. Ma, G. Liu, *J. Phys. Chem. C* **111**, 10404 (2007)
5. G. Boopathi, S.G. Raj, G.R. Kumar, R. Mohan, *Proc. Mater. Sci.* **6**, 1436 (2014). <https://doi.org/10.1016/j.mspro.2014.07.123>
6. Y.A. Kuznetsova, A.F. Zatsepin, *I.O.P. Conf. Ser. J. Phys. Conf. Ser.* **917**, 062001 (2017)
7. R.K. Tamrakar, D.P. Bisen, K. Upadhyay, I.P. Sahu, M. Sahu, *RSC Adv.* **6**, 92360 (2016)
8. R.K. Tamrakar, D.P. Bisen, N. Brahme, K. Upadhyay, *Optik* **126**, 2654 (2015)
9. R.K. Tamrakar, D.P. Bisen, K. Upadhyay, I.P. Sahu, *J. Alloys Compd.* **655**, 423 (2016)
10. M. Pokhrel, G.A. Kumar, D.K. Sardar, *J. Mater. Chem. A* **1**, 11595 (2013)
11. M.T. Man, H.S. Lee, *Sci. Rep.* **9**, 4613 (2019)
12. E. Hemmer, H. Takeshita, T. Yamano, T. Fujiki, Y. Kohl, K. Love, N. Venkatachalam, H. Hyodo, *J. Mater. Sci. Mater. Med.* **23**, 2399 (2012)
13. Y. Yang, J. Gu, R. Yang, Q. Shang, J. Yang, *Nanosci. Nanometrol.* **2**, 41 (2016)
14. E. Matijevic, W. Hsu, *J. Colloid, Interface Sci.* **118**, 506 (1987)
15. R. Li, L. Li, Y. Han, S. Gai, F. He, P. Yang, *J. Mater. Chem. B.* **2**, 2127 (2014)
16. W. Di, X. Ren, L. Zhang, C. Liu, S. Lu, *Cryst. Eng. Commun.* **13**, 4831 (2011)
17. K.M. Lin, C.C. Lin, Y.Y. Li, *Nanotechnology* **17**, 1745 (2006)
18. H. Xiao, P. Li, F. Jia, L. Zhang, *J. Phys. Chem. C* **113**, 21034 (2009)
19. L.Q. Minh, T.K. Anh, N.D. Hung, P.T.M. Chau, N.T.Q. Hai, H.V. Tuyen, V.T.T. Ha, V.D. Tu, W. Streck, *J. Rare Earth* **37**, 1126 (2019)
20. W. Song, W. Di, W. Qin, *Dalton Trans.* **45**, 7443 (2016)
21. T.K. Anh, N.T. Huong, P.T. Lien, D.K. Tung, V.D. Tu, N.D. Van, W. Streck, L.Q. Minh, *Mater. Sci. Eng. B* **241**, 1 (2019)
22. S.K. Raniyal, A.K. Soni, V.K. Rai, *Methods Appl. Fluorsc.* **5**, 035004 (2017)
23. A. Vosk, A. Saar, *Nanoscale Res. Lett.* **9**, 47 (2014)
24. R.K. Tamrakar, D.P. Bisen, K. Upadhyay, N. Brame, *Superlattice Microstruct.* **81**, 34 (2015)
25. S. Xu, D. Fang, Z. Zhang, Z. Jiang, *J. Solid State Chem.* **178**, 2159 (2005)

**Publisher's Note** Springer Nature remains neutral with regard to jurisdictional claims in published maps and institutional affiliations.